ORIGINAL ARTICLE

JBMR®

Identification of *IDUA* and *WNT16* Phosphorylation-Related Non-Synonymous Polymorphisms for Bone Mineral Density in Meta-Analyses of Genome-Wide Association Studies

Tianhua Niu,[1*] Ning Liu,[2*] Xun Yu,[2] Ming Zhao,[1] Hyung Jin Choi,[3,4] Paul J Leo,[5] Matthew A Brown,[5] Lei Zhang,[1,6] Yu-Fang Pei,[1] Hui Shen,[1] Hao He,[1] Xiaoying Fu,[1] Shan Lu,[2] Xiang-Ding Chen,[2] Li-Jun Tan,[2] Tie-Lin Yang,[7] Yan Guo,[7] Nam H Cho,[8] Jie Shen,[9] Yan-Fang Guo,[9] Geoffrey C Nicholson,[10] Richard L Prince,[11,12] John A Eisman,[13] Graeme Jones,[14] Philip N Sambrook,[15] Qing Tian,[1] Xue-Zhen Zhu,[7] Christopher J Papasian,[16] Emma L Duncan,[5,17] André G Uitterlinden,[18,19,20] Chan Soo Shin,[3] Shuanglin Xiang,[2] and Hong-Wen Deng[1,2]

[1]Department of Biostatistics and Bioinformatics, School of Public Health and Tropical Medicine, Tulane University, New Orleans, LA, USA
[2]College of Life Science, Hunan Normal University, Changsha, P.R. China
[3]Department of Internal Medicine, College of Medicine, Seoul National University, Seoul, Korea
[4]Department of Internal Medicine, Chungbuk National University Hospital, Cheongju, Korea
[5]University of Queensland Diamantina Institute, Translational Research Institute, Princess Alexandra Hospital, Brisbane, Australia
[6]Center of System Biomedical Sciences, University of Shanghai for Science and Technology, Shanghai, P.R. China
[7]School of Life Science and Technology, Xi'an Jiaotong University, Xi'an, P.R. China
[8]Department of Preventive Medicine, Ajou University School of Medicine, Youngtong-Gu, Korea
[9]Third Affiliated Hospital of Southern Medical University, Guangzhou, P.R. China
[10]School of Medicine, The University of Queensland, Toowoomba, Australia
[11]School of Medicine and Pharmacology, University of Western Australia, Perth, Australia
[12]Department of Endocrinology and Diabetes, Sir Charles Gairdner Hospital, Perth, Australia
[13]Garvan Institute of Medical Research, University of New South Wales, Sydney, Australia
[14]Menzies Institute for Medical Research, University of Tasmania, Hobart, Australia
[15]Kolling Institute of Medical Research, Royal North Shore Hospital, University of Sydney, Sydney, Australia
[16]Department of Basic Medical Science, University of Missouri–Kansas City, Kansas City, MO, USA
[17]Department of Endocrinology, Royal Brisbane and Women's Hospital, Brisbane, Australia
[18]Department of Internal Medicine, Erasmus Medical Center, Rotterdam, The Netherlands
[19]Department of Epidemiology, Erasmus Medical Center, Rotterdam, The Netherlands
[20]Netherlands Genomics Initiative (NGI)-sponsored Netherlands Consortium for Healthy Aging (NCHA), Leiden, The Netherlands

ABSTRACT

Protein phosphorylation regulates a wide variety of cellular processes. Thus, we hypothesize that single-nucleotide polymorphisms (SNPs) that may modulate protein phosphorylation could affect osteoporosis risk. Based on a previous conventional genome-wide association (GWA) study, we conducted a three-stage meta-analysis targeting phosphorylation-related SNPs (phosSNPs) for femoral neck (FN)-bone mineral density (BMD), total hip (HIP)-BMD, and lumbar spine (LS)-BMD phenotypes. In stage 1, 9593 phosSNPs were meta-analyzed in 11,140 individuals of various ancestries. Genome-wide significance (GWS) and suggestive significance were defined by $\alpha = 5.21 \times 10^{-6}$ (0.05/9593) and 1.00×10^{-4}, respectively. In stage 2, nine stage 1–discovered phosSNPs (based on $\alpha = 1.00 \times 10^{-4}$) were in silico meta-analyzed in Dutch, Korean, and Australian cohorts. In stage 3, four phosSNPs that replicated in stage 2 (based on $\alpha = 5.56 \times 10^{-3}$, 0.05/9) were de novo genotyped in two independent cohorts. *IDUA* rs3755955 and rs6831280, and *WNT16* rs2707466 were associated with BMD phenotypes in each respective stage, and in three stages combined, achieving GWS for both FN-BMD ($p = 8.36 \times 10^{-10}$, $p = 5.26 \times 10^{-10}$, and $p = 3.01 \times 10^{-10}$, respectively) and HIP-BMD ($p = 3.26 \times 10^{-6}$, $p = 1.97 \times 10^{-6}$, and $p = 1.63 \times 10^{-12}$, respectively). Although in vitro studies demonstrated no differences in expressions of wild-type and mutant forms of

Received in original form January 23, 2015; revised form July 29, 2015; accepted August 6, 2015. Accepted manuscript online August 8, 2015.
Address correspondence to: Hong-Wen Deng, PhD, Department of Biostatistics and Bioinformatics, Center for Bioinformatics and Genomics, Tulane University School of Public Health and Tropical Medicine, 1440 Canal Street, Suite 2001, New Orleans, LA 70112, USA. E-mail: hdeng2@tulane.edu
*TN and NL contributed equally to this work.
Additional Supporting Information may be found in the online version of this article.

Journal of Bone and Mineral Research, Vol. 31, No. 2, February 2016, pp 358–368
DOI: 10.1002/jbmr.2687

IDUA and WNT16B proteins, in silico analyses predicts that *WNT16* rs2707466 directly abolishes a phosphorylation site, which could cause a deleterious effect on WNT16 protein, and that *IDUA* phosSNPs rs3755955 and rs6831280 could exert indirect effects on nearby phosphorylation sites. Further studies will be required to determine the detailed and specific molecular effects of these BMD-associated non-synonymous variants. © 2015 American Society for Bone and Mineral Research.

KEY WORDS: OSTEOPOROSIS; HUMAN ASSOCIATION STUDIES; SINGLE-NUCLEOTIDE POLYMORPHISM; META-ANALYSIS WNT/BETA-CATENIN/LRPS

Introduction

Osteoporosis, a complex disease characterized by reduced bone mass, results in microarchitectural deterioration of bone tissue, and increased bone fragility and susceptibility to fracture.[1] It has been estimated that the prevalence of osteoporosis in the United States will increase to >14 million people in 2020,[2] and by 2025 it is projected that there will be >3 million fractures/year in the United States, costing $25.3 billion annually.[3] A diagnosis of osteoporosis for both males and females is attained when bone mineral density (BMD) is 2.5 SD or more below the young adult mean.[4] BMD, a highly heritable polygenic trait, is the best predictor for skeletal fragility.[5]

Protein phosphorylation represents the most widespread posttranslational modification (PTM) that plays a critical role in essential cellular processes; eg, metabolism, cell signaling, differentiation, and membrane transportation.[6] Large-scale phosphoproteomics studies suggest that more than one-half of all eukaryotic proteins are phosphorylated.[7] The most common phosphorylation sites in eukaryotes are serine (S), threonine (T), and tyrosine (Y) residues,[8] which are catalyzed by S/T-specific, Y-specific, and dual-specificity protein kinases.[9] Single-nucleotide polymorphisms (SNPs) constitute almost 90% of genetic variations in the human genome.[10] Non-synonymous SNPs (nsSNPs), defined as SNPs resulting in amino acid changes that include either missense or nonsense mutations,[11] represent 60% of known disease-causing mutations.[12] Of the nsSNPs, those that create/alter/abolish phosphorylation sites, called phosphorylation-related SNPs (phosSNPs), have been recognized as functional variants for a spectrum of human diseases; eg, lung cancer (*CSF1R* rs10079250),[13] prostate cancer (*TP53* rs1042522),[13,14] long QT syndrome (*KCNH2* rs1805123),[15,16] systemic lupus erythematosus (*VEGR2* rs2305948),[17] and tuberculosis (*TLR2* rs5743708).[18,19] Each phosphorylation site consists of an acceptor residue surrounded by an evolutionarily conserved motif consisting of seven to 12 amino acid residues on either flanking region. Based on the hypothesis that a sequence motif surrounding an acceptor residue represents a main determinant of protein kinase specificity, phosphorylation sites can be predicted in silico, and nsSNPs affecting such sites can be identified. From 91,797 nsSNPs from the National Center for Biotechnology Information (NCBI)'s dbSNP Build 130, by applying the Group-based Phosphorylation Scoring (GPS) 2.0 program (a kinase-specific phosphorylation site predictor),[20] Ren and colleagues[21] identified 64,035 phosSNPs residing in 17,614 human proteins, which were categorized into five distinct types based on the different effects they exert on phosphorylation sites: types I, II, III, IV, and V.

Among at least 60 loci identified by >40 previous genome-wide association (GWA) studies and meta-analyses of these studies for osteoporosis, the *WNT16* locus has been found to be an important genetic determinant of osteoporosis risk.[22] The human *WNT16* gene spans ~16 kb from initiation to termination codons, encoding two protein isoforms: WNT16A (40.5 kD) and WNT16B (40.7 kD).[23] As depicted in Supporting Fig. 1, these two WNT16 isoforms have different first exons (ie, 1a and 1b, respectively), independently controlled by two alternative promoters P1 and P2, respectively.[24] Expression of the WNT16A isoform has been shown to be restricted to the pancreas in humans, whereas WNT16B is expressed in multiple organs.[24] Compared to WNT16A, the role of WNT16B as a key regulator of osteoclastogenesis has been more extensively characterized.[25]

Meta-analyses of GWA studies have significant potentials for detecting subtle genetic effects.[26] However, because conventional GWA studies often include a large number of variants of unknown functional effects, the significance threshold attained by Bonferroni correction becomes overly conservative, producing a high rate of type II error (ie, β). PhosSNPs are more likely disruptive to protein function than other protein-coding missense mutations.[27] However, such potentially causal missense mutations could be missed by conventional GWA approaches because of very strict control for type I error (ie, α). Power to detect disease-causing variants can thus be increased by focusing exclusively on SNPs with higher prior probabilities of functional effects, either as in a whole-exome sequencing[28] approach targeting solely exonic SNPs, or as we apply here, targeting exclusively potentially functional phosSNPs. However, such a functional candidate genomic region approach[29] could be susceptible to a higher rate of false-positive results.[30] Therefore, to guard against an inflated α, we employed a three-stage approach, such that those phosSNPs attaining genome-wide significance (GWS) in stage 1 (ie, GWA discovery) are required to be replicated in independent cohorts of stages 2 and 3, respectively, based on their corresponding Bonferroni-corrected α thresholds.

Materials and Methods

A detailed description of study participants, phenotype measurement and modeling, DNA genotyping, quality control (QC), genotype imputation, association tests, meta-analysis methods, and regional association plots of the three-stage GWA meta-analysis is given in the Supporting Materials and Methods. At stage 1, seven GWA cohorts were included, and a suggestive significance threshold of $\alpha = 1.00 \times 10^{-4}$ was applied for phosSNP selection. At stage 2 (in silico replication), three GWA cohorts were included, and at stage 3 (de novo genotyping replication), two independent cohorts were included, and at each stage a Bonferroni-corrected significance threshold was applied.

PhosSNPs in potential phosphorylation sites

The phosSNP-centric GWA meta-analysis focuses exclusively on 9593 phosSNPs in stage 1 of the conventional GWA meta-analysis.[31] Details about phosSNP selection are given in the Supporting Materials and Methods.

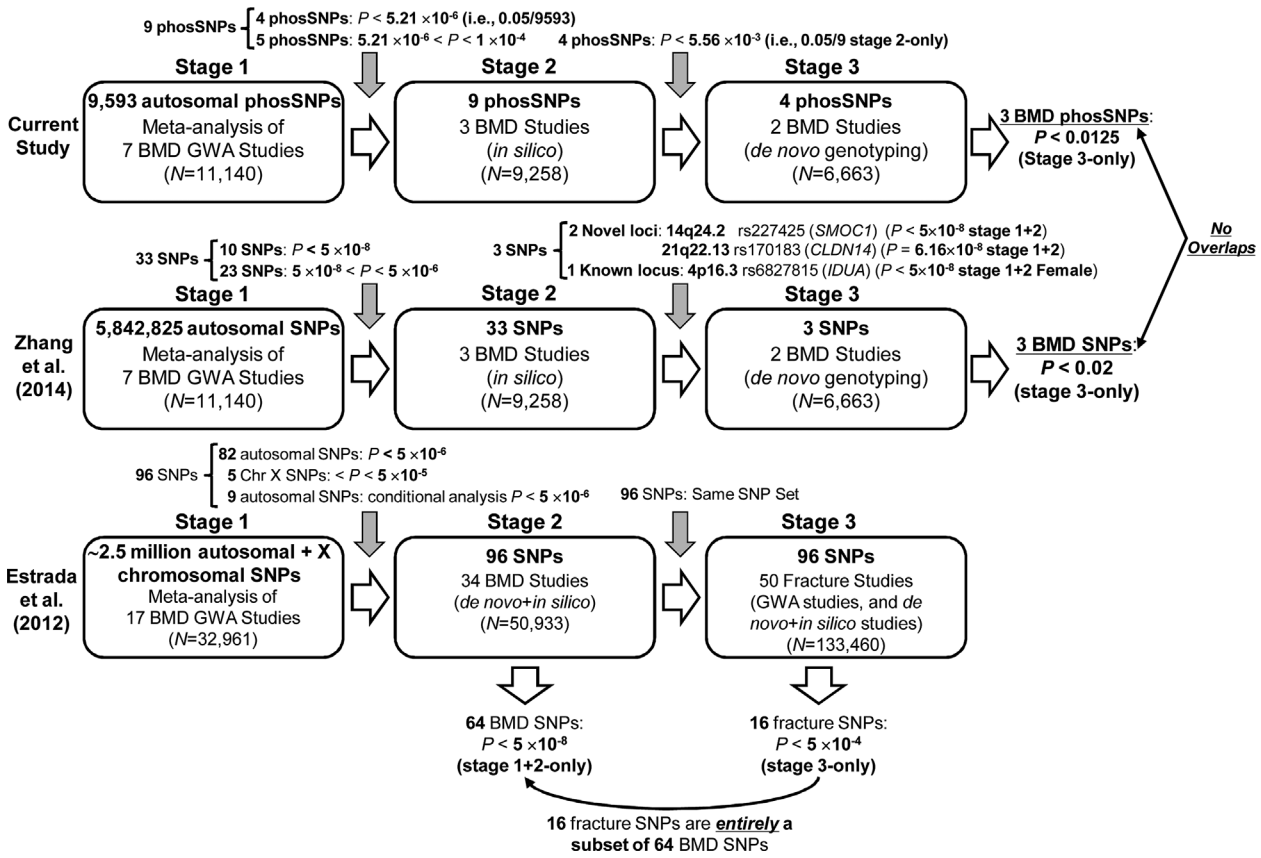

Fig. 1. Diagrammatic representations of study designs of three-stage GWA meta-analysis of current study (top panel), Zhang and colleagues[31] (middle panel), and Estrada and colleagues[41] (bottom panel).

In silico bioinformatics analyses

Computational predictions of phosphorylation sites affected by phosSNPs

Phosphorylation sites that could be affected by the three significant phosSNPs—*IDUA* rs3755955 (R105Q) and rs6831280 (A361T), and *WNT16* rs2707466 (WNT16B T263I)—were predicted by two commonly used online software programs: NetPhos2.0[32] and NetPhosK1.0.[33] Details about these programs are given in the Supporting Materials and Methods.

Computational predictions of functional impacts of phosSNPs

Functional effects of the three significant phosSNPs—*IDUA* rs3755955 (R105Q) and rs6831280 (A361T), and *WNT16* rs2707466 (WNT16B T263I)—were computed using four online software tools: (1) Mutation Assessor[34]; (2) BLOSUM62[35]; (3) PMut[36]; and (4) PANTHER.[37] Details about these tools are given in the Supporting Materials and Methods.

Computational prediction of protein secondary and tertiary structures

Protein secondary and tertiary structures were predicted by Protein Homology/analogy Recognition Engine Version 2.0 (Phyre^2).[38,39] The Phyre^2 server predicts a protein's secondary structure based on the amino acid sequence. In brief, this program converts a protein sequence into a hidden Markov model (HMM) based on sequence homologs retrieved from experimentally determined known protein structures using PSI-Blast.[40] The HMM of the query sequence is then scanned against a nonredundant library of HMMs of proteins with experimentally determined structures. The 3D model of the query sequence is then constructed on the basis of alignments between the HMM of the query sequence and the HMMs of known structures. Phyre^2 program can generate highly accurate models at low sequence identities (eg, 15% to 25%).[39]

In vitro protein expression studies

To assess whether mutant (MUT) alleles of respective phosSNPs, ie, *IDUA* rs3755955, rs6831280, and *WNT16* rs2707466, could affect protein expression levels in vitro, we designed and constructed plasmid pcDNA3.1-Myc/His vectors harboring either wild-type (WT) or MUT allele of each phosSNP and transfected each of them into Chinese hamster ovary (CHO) cells. Details about cloning and transfection and Western blot analyses are given in the Supporting Materials and Methods.

Results

Cohort characteristics at three stages were presented in Supporting Table 1. A detailed comparison of study designs of current study with those of two previous conventional GWA meta-analysis studies[31,41] is shown in Fig. 1. In stage 1, the current study restricted association tests to exclusively

Table 1. Comparison of 33 SNPs (Previous Conventional Study[31]) and 9 PhosSNPs (Current Study) Selected in Stage 1

Stage 1 of Zhang and colleagues[31] (2014)						Stage 1 of current study					
SNP ID	Locus	Gene	Phenotype	Analysis	*p*	SNP ID	Locus	Gene	Phenotype	Analysis	*p*
rs34920465	**1p36.12**	***ZBTB40***	**HIP-BMD**	**Combined**	**3.06×10^{-9}**	—	—	—	—	—	—
rs1430740	**1p31.3**	***MIR1262***	**LS-BMD**	**Combined**	**8.46×10^{-9}**	—	—	—	—	—	—
rs11582394	1q32.1	*PLEKHA6*	FN-BMD	Combined	7.14×10^{-7}	—	—	—	—	—	—
rs11696050	**2q34**	***PTH2R***	**HIP-BMD**	**Combined**	**3.72×10^{-8}**	—	—	—	—	—	—
rs11130082	3p21.31	*FYCO1*	LS-BMD	Combined	9.73×10^{-7}	—	—	—	—	—	—
rs6827815	4p16.3	*FGFRL1*	FN-BMD	Combined	6.01×10^{-7}	rs6831280	4p16.3	*IDUA*	FN-BMD	Combined	1.21×10^{-6}
						rs3755955	4p16.3	*IDUA*	FN-BMD	Combined	1.80×10^{-6}
rs17813558	4p16.1	*PSAPL1*	FN-BMD	Combined	9.19×10^{-7}	—	—	—	—	—	—
rs4974930	4p14	*WDR19*	HIP-BMD	Combined	6.20×10^{-7}	—	—	—	—	—	—
rs1463104	4q22.1	*HSP90AB3P*	LS-BMD	Combined	7.08×10^{-7}	rs1054627	4q22.1	*IBSP*	FN-BMD	Female	3.54×10^{-7}
rs4703541	5q13.2	*ZNF366*	FN-BMD	Combined	6.52×10^{-7}	—	—	—	—	—	—
rs6894139	**5q14.3**	***MEF2C***	**FN-BMD**	**Combined**	**2.02×10^{-9}**	—	—	—	—	—	—
—	—	—	—	—	—	rs61748601	6p21.2	*DNAH8*	HIP-BMD	Combined	4.83×10^{-5}
rs1871859	**6q25.1**	***C6orf97***	**LS-BMD**	**Female**	**5.04×10^{-9}**	—	—	—	—	—	—
rs28529426	7p22.1	*FOXK1*	LS-BMD	Combined	8.12×10^{-7}	—	—	—	—	—	—
rs2529750	7p21.1	*PRPS1L1*	LS-BMD	Female	7.04×10^{-7}	—	—	—	—	—	—
rs10429035	**7q21.3**	***FLJ42280***	**HIP-BMD**	**Combined**	**4.24×10^{-9}**	—	—	—	—	—	—
rs13242054	7q22.3	*PIK3CG*	LS-BMD	Combined	5.83×10^{-7}	—	—	—	—	—	—
rs10242100	**7q31.31**	***WNT16***	**HIP-BMD**	**Combined**	**4.63×10^{-8}**	rs2707466	7q31.31	*WNT16*	HIP-BMD	Combined	1.77×10^{-6}
chr8:78734104	8q21.12	*PKIA*	LS-BMD	Combined	1.98×10^{-7}	—	—	—	—	—	—
rs4424296	**8q24.12**	***TNFRSF11B***	**LS-BMD**	**Combined**	**5.94×10^{-10}**	—	—	—	—	—	—
rs10868819	9q21.12	*KLF9*	FN-BMD	Combined	6.31×10^{-7}	—	—	—	—	—	—
chr9:87907046	9q21.33	*AGTPBP1*	HIP-BMD	Male	1.88×10^{-7}	—	—	—	—	—	—
rs7025969	9q31.3	*ACTL7B*	FN-BMD	Female	7.77×10^{-8}	—	—	—	—	—	—
rs7108738	**11p15.1**	***SOX6***	**FN-BMD**	**Combined**	**6.73×10^{-9}**	—	—	—	—	—	—
rs4267051	11p15.1	*HPS5*	HIP-BMD	Female	7.97×10^{-7}	—	—	—	—	—	—
rs525592	11q13.2	*LRP5*	LS-BMD	Combined	9.04×10^{-7}	—	—	—	—	—	—
rs471753	11q14.2	*TMEM135*	FN-BMD	Combined	2.20×10^{-7}	—	—	—	—	—	—
—	—	—	—	—	—	rs1318648	12q13.13	*ESPL1*	FN-BMD	Female	9.87×10^{-5}
—	—	—	—	—	—	rs56358776	12q13.13	*ESPL1*	FN-BMD	Combined	5.36×10^{-5}
rs9533095	13q14.11	*AKAP11*	LS-BMD	Female	3.96×10^{-7}	—	—	—	—	—	—
rs227425	14q24.2	*SMOC1*	LS-BMD	Combined	2.69×10^{-7}	—	—	—	—	—	—
rs11848357	14q32.11	*RPS6KA5*	LS-BMD	Combined	3.29×10^{-7}	—	—	—	—	—	—
chr16:86714715	**16q24.1**	***FOXL1***	**HIP-BMD**	**Female**	**1.86×10^{-9}**	—	—	—	—	—	—
rs10756	19q12	*C19orf2*	FN-BMD	Combined	7.60×10^{-7}	—	—	—	—	—	—
—	—	—	—	—	—	rs2287679	19q13.11	*GPATCH1*	FN-BMD	Female	6.59×10^{-5}
rs12481249	20q13.33	*OSBPL2*	LS-BMD	Combined	1.20×10^{-7}	rs310655	20q13.33	*SRMS*	FN-BMD	Combined	3.57×10^{-5}
rs170183	21q22.13	*CLDN14*	HIP-BMD	Female	3.71×10^{-7}	—	—	—	—	—	—

Combined refers to male and female. Those SNPs that have attained the conventional GWS (ie, $\alpha = 5.00 \times 10^{-8}$) are in bold. Shaded regions are matched regions between these two studies, although different SNPs were identified. (Note: a region can contain more than one SNP.)

SNP = single-nucleotide polymorphism; phosSNP = phosphorylation-related SNP; BMD = bone mineral density; HIP = total hip; LS = lumbar spine; FN = femoral neck; GWS = genome-wide significance.

phosSNPs (~10 K), as opposed to the entire set of genotyped and imputed SNPs (~5800 K) of a previous conventional study.[31] As a result, different SNP sets were selected from stage 1 for stage 2 in silico replication (nine phosSNPs for current study, and none overlapped with 33 SNPs of previous conventional study[31]). In stage 2, different SNP selection criteria were employed between the current study and the previous conventional study.[31] Four stage 2–selected phosSNPs (ie, *IDUA* rs3755955 and rs6831280, *WNT16* rs2707466, and *ESPL1* rs56358776) of the current study were entirely different from those three stage 2–selected SNPs of the previous conventional study[31] (ie, *SMOC1* rs227425, *CLDN14* rs170183, and intergenic SNP rs6827815).

Stage 1 (GWA discovery)

Table 1 presents a comparison of 33 SNPs selected in stage 1 of the previous conventional study,[31] with those nine phosSNPs selected in stage 1 of the current study, which include four phosSNPs (located in three gene regions) attaining phosSNP-centric GWS (ie, $\alpha = 0.05/9593 = 5.21 \times 10^{-6}$)—*IBSP* rs1054627 for FN-BMD in a female-specific sample, *IDUA* rs6831280 and rs3755955 for FN-BMD in a gender-combined (ie, male and female) sample, and *WNT16* rs2707466 for HIP-BMD in a gender-combined sample—and another five phosSNPs (located in four gene regions) attaining only suggestive significance (ie, $\alpha = 1.00 \times 10^{-4}$)—*SRMS* rs310655 for FN-BMD in a gender-combined sample, *DNAH8* rs61748601 for HIP-BMD in a gender-combined sample, *ESPL1* rs56358776 and rs1318648 for LS-BMD in gender-combined and female-specific samples, respectively, and *GPATCH1* rs2287679 for FN-BMD in a female-specific sample.

Stage 2 (in silico replication)

In stage 2, the above nine stage 1–discovered phosSNPs were subject to replication in three in silico independent cohorts. A meta-analysis within stage 2 revealed six phosSNPs at Bonferroni corrected $\alpha = 5.56 \times 10^{-3}$ (ie, 0.05/9)—*WNT16* rs2707466 for FN-BMD in a gender-combined sample, *IBSP* rs1054627 for FN-BMD in a gender-combined sample, *ESPL1* rs1318648 and rs56358776 for LS-BMD in a gender-combined sample, and *IDUA* rs3755955 and rs6831280 for FN-BMD in a gender-combined sample. Of these, *IBSP* encodes a well-known bone matrix protein that is important for bone mineralization[42–44] which, consequently, was not further tested in stage 3. For *ESPL1* phosSNPs rs1318648 and rs56358776, neither reached GWS (ie, $5.21 \times 10^{-6} \le p < 1.00 \times 10^{-4}$) in stage 1 phosSNP-centric GWA meta-analysis. *ESPL1* rs1318648 is a previously known nsSNP suggestively associated with FN-BMD and LS-BMD phenotypes,[41] whereas *ESPL1* rs56358776 is a novel nsSNP that was not reported in either of two previous conventional studies,[41,45] which is in high linkage disequilibrium (LD) with *ESPL1* rs1318648 ($r^2 = 0.798$ in 1000 Genomes [1KG] Pilot 1 CEU Population by applying the SNP Annotation and Proxy search [SNAP] tool[46] of the Broad Institute, Cambridge, MA, USA). Therefore, we selected four stage 2–replicated phosSNPs—*IDUA* rs6831280 and rs3755955, *WNT16* rs2707466, and potentially novel phosSNP *ESPL1* rs56358776—for stage 3 de novo genotyping replication.

Stage 3 (de novo genotyping replication)

In stage 3, the four stage 2–selected phosSNPs identified in the previous paragraph were subject to further replication by de novo genotyping. Three of these phosSNPs were replicated by stage 3–specific meta-analysis at Bonferroni corrected $\alpha = 0.0125$ (ie, 0.05/4). *WNT16* rs2707466 was consistently replicated for HIP-BMD, FN-BMD, and LS-BMD phenotypes in a gender-combined sample. *IDUA* rs3755955 and rs6831280 were significantly associated with FN-BMD and HIP-BMD phenotypes in a gender-combined sample. *ESPL1* rs56358776 was not replicated at this stage ($p = 0.79$, $p = 0.78$, and $p = 0.32$ in a gender-combined sample for FN-BMD, HIP-BMD, and LS-BMD, respectively).

Stage 1+2+3 meta-analysis

Table 2 presents ethnicity-specific and combined meta-analysis results aggregating these three stages for stage 1–discovered ($\alpha = 1.00 \times 10^{-4}$), stage 2–replicated, and stage 3–replicated (Bonferroni-corrected $\alpha = 5.56 \times 10^{-3}$ and 0.0125, respectively) phosSNPs: *IDUA* rs6831280 (A361T); *IDUA* rs3755955 (R105Q); and *WNT16* rs2707466 (WNT16B T263I), respectively. In ethnicity-specific meta-analyses, in whites, all three attained phosSNP-centric GWS (ie, $\alpha = 5.21 \times 10^{-6}$) for FN-BMD and only *WNT16* rs2707466 attained this threshold for HIP-BMD; and in Asians, only *WNT16* rs2707466 attained phosSNP-centric GWS for HIP-BMD. The effects of these phosSNPs were consistent between white and Asian ethnicities. In combined meta-analysis across three stages, *IDUA* rs3755955 was significantly associated with FN-BMD and HIP-BMD phenotypes ($p = 8.36 \times 10^{-10}$ and $p = 3.26 \times 10^{-6}$, respectively). Likewise, *IDUA* rs6831280 was significantly associated with FN-BMD and HIP-BMD phenotypes ($p = 5.26 \times 10^{-10}$ and $p = 1.97 \times 10^{-6}$, respectively). Similarly, *WNT16* rs2707466 was significantly associated with FN-BMD and HIP-BMD phenotypes ($p = 3.01 \times 10^{-10}$ and $p = 1.63 \times 10^{-12}$, respectively). Regional association plots were generated for these three significant phosSNPs—*IDUA* rs3755955 and rs6831280 (Fig. 2), and *WNT16* rs2707466 (Fig. 3).

Phosphorylation sites predicted to be affected by *IDUA* and *WNT16* phosSNPs

Based on predictions by the two in silico bioinformatics tools NetPhos2.0 and NetPhosK1.0, four phosphorylation sites were predicted to be affected by these three BMD-associated phosSNPs (either NetPhos2.0 score >0.5 or NetPhosK1.0 score >0.5) (Table 3). Detailed information on 96 and 54 predicted phosphorylation sites for IDUA and WNT16B are presented in Supporting Tables 2 and 3, respectively. IDUA phosphorylation sites T98 and S102 were potentially affected by their neighboring phosSNP *IDUA* rs3755955 (R105Q), whereas IDUA phosphorylation site T366 was potentially affected by a neighboring phosSNP *IDUA* rs6831280 (A361T). WNT16B phosphorylation site T263 was potentially directly abolished by phosSNP *WNT16* rs2707466 (WNT16B T263I). Of them, WNT16B T263 (affected by *WNT16* rs2707466) has been experimentally validated to be phosphorylated in vivo,[47] whereas IDUA T98 and S102 (potentially affected by *IDUA* rs3755955) and T366 (potentially affected by *IDUA* rs6831280) have yet not been experimentally confirmed.

Predicted functional impacts of *IDUA* and *WNT16* phosSNPs

As shown in Supporting Table 4, although *IDUA* rs6831280 (A361T) and rs3755955 (R105Q) were predicted to have no (Mutation Assessor and BLOSUM62 scores) or low (PMut and

Table 2. GWA Meta-Analysis Results of Stage 1+2+3 for BMD-Associated PhosSNPs in Ethnicity-Specific and Combined Cohorts

Gene symbol	SNP ID (WT/MUT alleles; AA change)	PhosSNP type	Phenotype		
			FN-BMD	HIP-BMD	LS-BMD
White (7 cohorts)					
IDUA	rs3755955 (G/A; R105Q)	Type II (+)	$\mathbf{2.38 \times 10^{-8}}$	2.34×10^{-4}	0.0188
IDUA	rs6831280 (G/A; A361T)	Type III	$\mathbf{1.98 \times 10^{-8}}$	1.83×10^{-6}	0.0366
WNT16	rs2707466 (C/T; T263I*)	Type I (–)	$\mathbf{1.13 \times 10^{-7}}$	$\mathbf{4.54 \times 10^{-7}}$	0.0109
Asian (3 cohorts)					
IDUA	rs3755955 (G/A; R105Q)	Type II (+)	0.03	0.0106	0.263
IDUA	rs6831280 (G/A; A361T)	Type III	0.033	0.0117	0.289
WNT16	rs2707466 (C/T; T263I*)	Type I (–)	1.20×10^{-3}	$\mathbf{1.04 \times 10^{-6}}$	6.67×10^{-3}
Total (12 cohorts)					
IDUA	rs3755955 (G/A; R105Q)	Type II (+)	$\mathbf{8.36 \times 10^{-10}}$	$\mathbf{3.26 \times 10^{-6}}$	8.50×10^{-3}
IDUA	rs6831280 (G/A; A361T)	Type III	$\mathbf{5.26 \times 10^{-10}}$	$\mathbf{1.97 \times 10^{-6}}$	0.0147
WNT16	rs2707466 (C/T; T263I*)	Type I (–)	$\mathbf{3.01 \times 10^{-10}}$	$\mathbf{1.63 \times 10^{-12}}$	1.17×10^{-4}

PhosSNPs attaining GWS level (ie, $p < 5.21 \times 10^{-6}$) are in bold. Combined refers to male and female. PhosSNP types are defined as follows: Type I (–), an nsSNP that removes the phosphorylation site; Type II (+), an nsSNP that creates one or multiple adjacent phosphorylation sites; and Type III, an nsSNP that induces changes of protein kinase type(s) at adjacent phosphorylation site(s) as defined in Ren and colleagues[21] (2010), which were predicted by GPS2.0 software.[20]

GWA = genome-wide association; BMD = bone mineral density; SNP = single-nucleotide polymorphism; phosSNP = phosphorylation-related SNP; WT = wild-type; MUT = mutant; AA = amino acid; FN = femoral neck; HIP = total hip; LS = lumbar spine; GWS = genome-wide significance; nsSNP = non-synonymous SNP.

*The amino acid position at WNT16B protein isoform (SWISS-PROT ID: Q9UBV4-1) is indicated.

PANTHER scores) functional impacts, *WNT16* rs2707466 (WNT16B T263I) showed the highest Mutation Assessor score (0.705, nearly reaching a "low impact" threshold 0.80), lowest BLOSUM62 score of (–1.00, indicative of "evolutionarily less acceptable"), highest PMut pathogenicity score (0.3099, indicative of a "moderate pathogenicity"), and lowest PANTHER subSPEC score (–1.92476, indicative of a deleterious effect corresponding to a highest deleteriousness probability $p_{\text{deleterious}} = 0.25441$). Further, evolutionary analyses by multiple sequence alignment method revealed that a 27–amino acid peptide (–14 to +12) surrounding the T263 phosphorylation site is conserved across three mammalian species—human, mouse and rat (Supporting Fig. 1)—supporting a likely functional significance of this phosSNP. Based on these bioinformatics

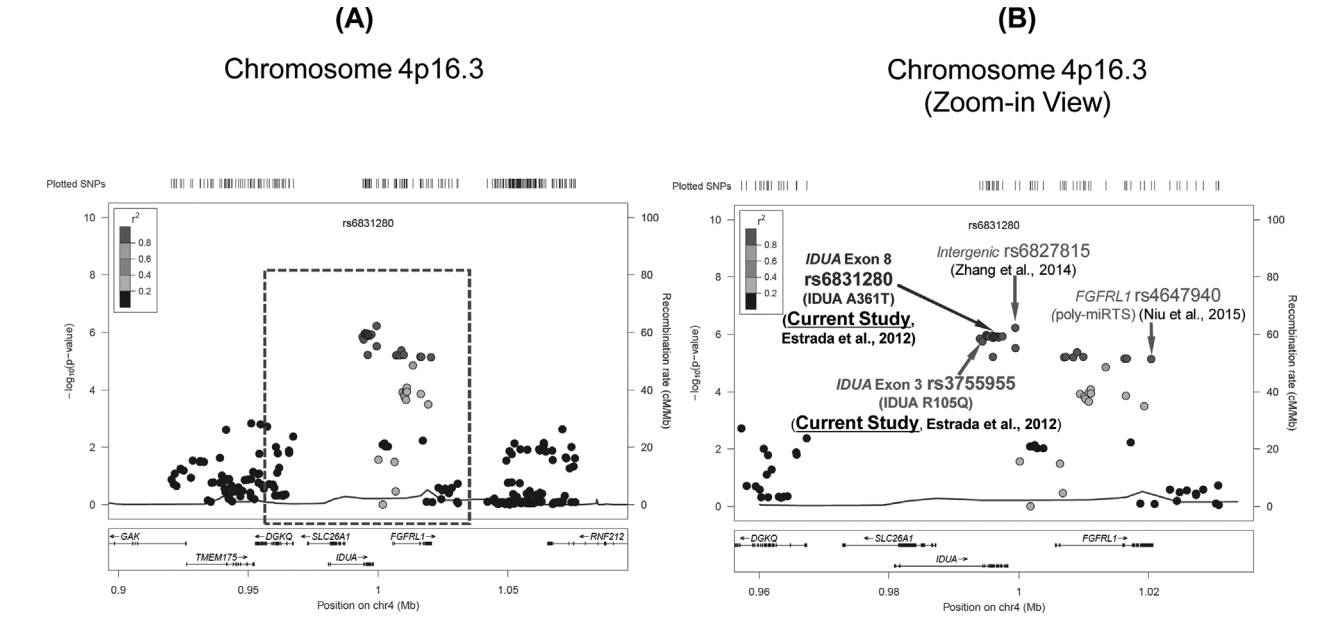

Fig. 2. Regional association plots for chromosome 4p16.3 loci *IDUA* exon 3 phosSNP rs3755955 (R105Q), exon 8 phosSNP rs6831280 (A361T), intergenic SNP rs6827815, and *FGFRL1* 3′-untranslated region SNP rs4647940 based on RefSeq accession number NG_008103.1 for FN-BMD (most significant phenotype). (*A*) *IDUA* rs6831280 with flanking ±100-kb (*B*) a zoomed-in view of the center region (indicated by the dashed box of *A*)—*IDUA* rs6831280 with flanking ±40-kb. PhosSNPs are highlighted in bold.

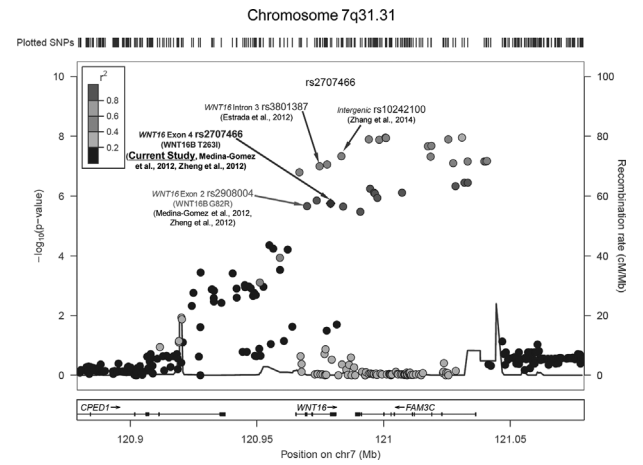

Fig. 3. Regional association plot for *WNT16* rs2707466 with flanking ±100-kb for HIP-BMD (most significant phenotype), with chromosome 7q31.31 *WNT16* exon 2 nsSNP rs2908004 (WNT16B, G82R), intron 3 SNP rs3801387, exon 4 phosSNP rs2707466 (WNT16B T263I), and intergenic SNP rs10242100 based on RefSeq accession number NG_029242.1 indicated. The phosSNP is highlighted in bold.

prediction results, we further assessed the potential impact of *WNT16* rs2707466 (WNT16B T263I) on WNT16B secondary and tertiary structures.

Predicted secondary and tertiary structures of WT and MUT alleles for *WNT16* phosSNP

The secondary and tertiary structures of protein isoforms encoded by WT and MUT alleles for *WNT16* rs2707466 (WNT16B T263I) predicted by the Phyre[2] server are presented in Supporting Figs. 2 and 3, respectively. With respect to secondary structures, this phosSNP (ie, T263 residue) is located in a disordered region (indicated by a tract of "?" symbols) typical for a phosphorylation site,[48] downstream of a predicted β-strand (SIQISDK) for either isoform (Supporting Fig. 2) with potential functional effects (Supporting Table 4). A comparison of the local 3D structures between WT and MUT isoforms near the T263 residue clearly shows different spatial patterns (Supporting Fig. 3, dashed boxes).

Effects of *IDUA* and *WNT16* phosSNPs on protein stability

In CHO cells, Western blot results showed that, at the protein level, *IDUA* rs6831280 (A361T) and rs3755955 (R105Q) MUT alleles were expressed at equivalent levels compared with the *IDUA* WT allele (Supporting Figs. 4A and 5A, respectively). The *WNT* rs2707466 (WNT16B T263I) MUT allele was also expressed at equivalent levels compared with the *WNT16* WT allele (Supporting Figs. 4B and 5B, respectively). Overall, the protein expression of the MUT allele is equivalent to that of the WT allele for each of these three phosSNPs, suggesting that their influences of protein phosphorylations could be important, rather than on expression levels per se.

Discussion

In the human genome, nsSNPs account for 60% of mutations that cause diseases.[12] However, not all nsSNPs lead to a functional impact. Therefore, it is essential to select only those nsSNPs that are most plausible causal variants. Our study is unique in associating phosSNPs affecting the most common type of PTM with BMD phenotypes by taking a three-stage approach to protect against an inflated false-positive rate. Beyond detecting genetic association, we also performed in silico and in vitro functional characterizations of identified significant nsSNPs. At stage 1, four chromosomal loci, ie, 4p16.3 (*IBSP*), 4q22.1 (*IDUA*), 7q31.31 (*WNT16*), and 20q13.33 (*GPATCH1*), were detected by both the current and conventional studies,[31] but were represented by totally different SNPs, and for 4q22.1 and 20q13.33 were represented by different genes. At 7q31.31, the previous study detected association with intergenic SNP rs10242100 (with no apparent functional significance) near *WNT16* gene, which is in moderate LD with the *WNT16* SNP rs2707466 detected by our current study ($r^2 = 0.462$ in 1KG Pilot

Table 3. In Silico Predicted Phosphorylation Sites of Three PhosSNPs Associated With BMD Phenotypes

Gene symbol	Predicted phosphorylation site (represented by PSP[7,7])	PhosSNP ID (WT/MUT alleles; AA change)	PhosSNP type	NetPhos2.0 score (prediction)	NetPhosK1.0 score (prediction)
IDUA	HWLLELV**T**TRGSTG***Q*** AA Pos: 98	rs3755955 (G/***A***; R105Q)	Type II (+)	0.417 (probable)	0.68 (yes)
IDUA	ELVTTRG**S**TG***Q***GLSY AA Pos: 102	rs3755955 (G/***A***; R105Q)	Type II(+)	0.987 (yes)	0.51 (yes)
IDUA	PF***T***QRTL**T**ARFQVNN AA Pos: 366	rs6831280 (G/***A***; A361T)	Type III	0.600 (yes)	0.51 (yes)
WNT16	SIQISDK***I***KRKMRRR AA Pos: 263[a]	rs2707466 (C/T; T263I**)	Type I (–)	0.833 (yes)	0.86 (yes)

PhosSNP types are defined as in the footnote of Table 2. The phosphorylation acceptor residue is underlined, and the phosSNP site (mutant allele shown) is highlighted in bold and italic. Predicted phosphorylation sites for respective phosSNPs have either a NetPhos2.0 score >0.5 or a NetPhosK1.0 score >0.5. GPS2.0 scores were directly extracted from the PhosSNP1.0 database,[21] where these scores were greater than their respective thresholds: 3.26, 2.85, and 2.43 for IDUA protein (SWISS-PROT ID: P35475) positions 98, 102, and 366, respectively; and 4.48 for WNT16B protein (SWISS-PROT ID: Q9UBV4-1) position 263. For NetPhos2.0 and NetPhosK1.0 scores, "Yes," "Probable," and "No" refer to a score >0.5, 0.1–0.5, and <0.1, respectively.

SNP = single-nucleotide polymorphism; phosSNP = phosphorylation-related SNP; BMD = bone mineral density; PSP = phosphorylation site peptide; WT = wild-type; MUT = mutant; AA = amino acid; NetPhos2.0 = neural network phosphorylation predictor; NetPhosK1.0 = neural network phosphorylation kinase-specific predictor; Pos = position.

[a]The amino acid position at WNT16B protein isoform (SWISS-PROT ID: Q9UBV4-1) is indicated.

1 CEU Population by applying SNAP tool[46]). Overall, three phosSNPs (*IDUA* rs6831280 and rs3755955, and *WNT16* rs2707466), were discovered in stage 1 and were independently replicated in stages 2 and 3, respectively. In ethnicity-specific meta-analyses, their effects were consistent in subgroups of white and Asian ancestries, and statistical significances were greater in white than in Asian samples in part because of a larger white sample size (Table 2). In combined stage 1+2+3 meta-analysis, all three phosSNPs reached conventional GWS for FN-BMD, and *WNT16* rs2707466 also attained conventional GWS for HIP-BMD. Applying NetPhos2.0 and NetPhosK1.0, there were 96 and 54 predicted phosphorylation sites in IDUA and WNT16B proteins, respectively (Supporting Tables 3 and 4). *IDUA* encodes a glycosyl hydrolase that hydrolyzes the terminal alpha-L-iduronic acid residues of two glycosaminoglycans, dermatan sulfate and heparan sulfate.[49] Wang and colleagues[50] created the Idua-W392X mouse model, and found that 35-week-old homozygous Idua-W392X mice showed a 24% increase in femur BMD, and bone abnormalities such as thickening of the zygomatic arch and aberrations in the length and width of the femur were also observed.

For IDUA protein, a predicted phosphorylation site, T366, could be indirectly affected by *IDUA* rs6831280 (A361T), a type III phosSNP, and two predicted phosphorylation sites, T98 and S102, could be indirectly affected by *IDUA* rs3755955 (R105Q), a type II (+) phosSNP (Table 3). For WNT16B protein, phosphorylation site T263 could be directly abolished by *WNT16* rs2707466 (WNT16B T263I), a type I (–) phosSNP. Of them, only WNT16B T263 has been experimentally validated to be a genuine phosphorylation site by mass spectrometry technology in a phosphoproteomic analyses of human embryonic stem cells in vivo.[47] Whether IDUA T98 and S102, and IDUA T366 are actual phosphorylation sites influenced by nearby *IDUA* phosSNPs rs3755955 (R105Q) and rs6831280 (A361T), respectively, remains to be experimentally determined.

WNT16 encodes a member of the wingless-type mouse mammary tumor virus (MMTV) integration site family, which has been reported to mediate signaling via both canonical and noncanonical Wnt pathways. Wnt proteins are known to play important roles in vertebrate skeletal development.[51–53] Wnt16 is expressed in osteoid tissue of craniofacial bones during embryonic development in mice, and suppresses osteoblast differentiation through the canonical β-catenin pathway in MC3T3-E1 preosteoblasts.[54] Several GWA meta-analysis studies have demonstrated that *WNT16* intron 3 SNP rs3801387,[41] exon 2 rs2908004 (WNT16B G82R), and exon 4 rs2707466 (WNT16B T263I),[55,56] as well as intergenic SNP rs10242100[31] are associated with BMD phenotypes (Fig. 3). However, functional roles of noncoding SNPs rs10242100 and rs3801387, which are in almost perfect LD ($r^2 = 0.915$ in 1KG Pilot 1 CEU Population by applying SNAP tool[46]), remain unclear. *WNT16* exon 2 rs2908004 (WNT16B G82R) and exon 4 rs2707466 (WNT16B T263I) are shown to be in nearly complete LD ($r^2 = 0.933$ in 1KG Pilot 1 CEU Population by applying SNAP tool[46]), which could represent the same phosphorylation association signal (ie, *WNT16* rs2707466). Consistent with our results, exon 2 nsSNP rs2908004 was significantly associated with upper limb BMD, lower limb BMD, as well as skull BMD phenotypes, and is the top signal in the chromosome 7q31.31 region in a GWA meta-analysis of the Avon Longitudinal Study of Parents and their Children and Generation R Study.[57] The phosSNP *WNT16* rs2707466 results in a substitution of threonine by isoleucine in both WNT16A (amino acid position 253) and WNT16B (amino acid position 263) isoforms. This phosSNP is predicted to exert a modest impact on protein function (by Mutation Assessor), and to be evolutionarily less acceptable (by BLOSUM62) and moderately deleterious (by PMut and PANTHER) (Supporting Table 4). Because WNT16B T263 has been experimentally confirmed to be a phosphorylation site in vivo,[47] in silico secondary structure prediction shows that T263 is located in a disordered region (Supporting Fig. 2). This is in agreement with findings of Dephoure and colleagues,[58] who showed that phosphorylation sites mostly occur in disordered regions, and the addition of a phosphate group to acceptor residue upon phosphorylation can lead to a disorder-to-order transition.[59] Predicted local 3D structures also indicate notable differences between WT and MUT isoforms around T263 phosphorylation site (Supporting Fig. 3). Taken together, it is highly probable that T263, a phosphorylatable residue located in a disordered region of WNT16B protein, acts as a switch for regulating protein-protein interactions,[59] and *WNT16* rs2707466, a type I (–) phosSNP that abolishes this phosphorylation site, constitutes a causal variant for BMD phenotype. This is supported by observations of *wnt16*-null mice, which had significantly reduced total body BMD, thinner cortical bones at the femur midshaft, and reduced bone strength of both the femur and tibia.[55,56] Further, local injection of WNT16B (WT form) could increase BMD, providing direct experimental evidence that the *WNT16* gene is critical for skeletal development.[25]

There are several limitations to our study. First, 9593 phosSNPs included in stage 1 (GWA discovery) of the current study represent 14.98% of the entire 64,035 phosSNP set. Nevertheless, the original 5,842,825 autosomal SNPs either directly-typed or imputed in stage 1 of the conventional GWA study[31] only covered 15.92% of the entire 36.7 million human autosomal SNP set.[60] Therefore, although these included phosSNPs appear limiting, they constitute a similar proportion of total phosSNPs as the original stage 1 SNP set of the previous conventional study.[31] Second, our in vitro protein expression experiments of WT and MUT alleles of *IDUA* rs3755955 (R105Q), rs6831280 (A361T), and *WNT16* rs2707466 (WNT16B T263I) *only* showed relatively equivalent protein expression levels between WT and MUT alleles (Supporting Figs. 4B and 5B, respectively). Additional experiments applying phosphospecific antibodies could be insightful to reveal whether these phosSNPs truly affect protein phosphorylations either *directly* (for *WNT16* phosSNP rs2707466) or *indirectly* (for *IDUA* phosSNP rs6831280 and rs3755955). However, such experiments are time-consuming and the extents of such differences may be challenging to detect, because both IDUA and WNT16B proteins can have multiple phosphorylation sites, and these phosSNPs may only affect one or two among them. It also remains to be shown whether a fraction of BMD variation is attributed to impacts of *IDUA* rs6831280 (A361T) and rs3755955 (R105Q) on their neighboring IDUA putative phosphorylation sites T98, S102, and T366, and to abolishment of the WNT16B T263 phosphorylation site by *WNT16* rs2707466 (WNT16B T263I). Nevertheless, the study of Movérare-Skrtic and colleagues[25] clearly showed a pivotal role of the WNT16B WT isoform in skeletal development, and phosSNP rs2707466 could indeed play a major functional role in regulating bone metabolism.

The collective findings from our multistage phosSNP-centric GWA meta-analysis identified and robustly validated three phosSNPs, *IDUA* rs6831280, *IDUA* rs3755955, and *WNT16* rs2707466, to be significantly associated with FN-BMD and HIP-BMD. These results could offer new mechanistic insights of

causal variants for osteoporosis. Because there is currently a lack of bone-specific phosphorylation maps for those phosphorylation sites that are impacted by these BMD-associated phosSNPs, more studies are necessary to elucidate whether phosphorylations affected by them are present in various types of bone cells, such as osteocytes, osteoblasts, and osteoclasts

Disclosures

All authors state that they have no conflicts of interest.

Acknowledgments

This study was partially supported by the Shanghai Leading Academic Discipline Project (S30501) and a startup fund from Shanghai University of Science and Technology. The investigators of this work were also supported by grants from the NIH (P50AR055081, R01AG026564, R01AR050496, RC2DE020756, R01AR057049, and R03TW008221), the Franklin D. Dickson/Missouri Endowment, and the Edward G. Schlieder Endowment. We thank Dr. Karol Estrada and Dr. Fernando Rivadeneira (both from Department of Internal Medicine and Department of Epidemiology, Erasmus Medical Center, Rotterdam, The Netherlands) for their help with analyzing and delivering the Rotterdam Study data. The Framingham Heart Study (FHS) is conducted and supported by the National Heart, Lung, and Blood Institute (NHLBI) in collaboration with Boston University (Contract Number N01-HC-25195). This manuscript was not prepared in collaboration with investigators of FHS and does not necessarily reflect the opinions or views of FHS, Boston University, or NHLBI. Funding for SHARe genotyping was provided by NHLBI Contract N02-HL-64278. SHARe Illumina genotyping was provided under an agreement between Illumina and Boston University. Funding support for the Framingham Bone Mineral Density datasets was provided by NIH grants R01 AR/AG 41398, R01 AR050066, and R03 AG20321.

Funding support for the Genetic Determinants of Bone Fragility was provided through the NIH National Institute of Aging (NIA) Division of Geriatrics and Clinical Gerontology. Genetic Determinants of Bone Fragility is a genome-wide association study funded as part of the NIA Division of Geriatrics and Clinical Gerontology. Assistance with phenotype harmonization and genotype cleaning, as well as with general study coordination, was provided by the NIA Division of Geriatrics and Clinical Gerontology and the NIA Division of Aging Biology. Support for the collection of datasets and samples were provided by the parent grant, Genetic Determinants of Bone Fragility (P01-AG018397). Funding support for the genotyping that was performed at the Johns Hopkins University Center for Inherited Diseases Research was provided by the NIH NIA.

The Women's Health Initiative (WHI) program is funded by the NHLBI, NIH, U.S. Department of Health and Human Services through contracts N01WH22110, 24152, 32100-2, 32105-6, 32108-9, 32111-13, 32115, 32118-32119, 32122, 42107-26, 42129-32, and 44221. This manuscript was not prepared in collaboration with investigators of the WHI, has not been reviewed and/or approved by WHI, and does not necessarily reflect the opinions of the WHI investigators or the NHLBI. WHI Population Architecture Using Genomics and Epidemiology (PAGE) is funded through the National Human Genome Research Institute (NHGRI) PAGE network (U01 HG004790). Assistance with phenotype harmonization, SNP selection, data cleaning, meta-analyses, data management and dissemination, and general study coordination, was provided by the PAGE Coordinating Center (U01HG004801-01). The FHS datasets used for the analyses described in this manuscript were obtained from dbGaP at http://www.ncbi.nlm.nih.gov/sites/entrez?db:gap through dbGaP accession phs000007.v14.p6. Assistance with phenotype harmonization and genotype cleaning, as well as with general study coordination, of Genetic Determinants of Bone Fragility study was provided by the NIA Division of Geriatrics and Clinical Gerontology and the NIA Division of Aging Biology. The Indiana Fragility Study (IFS) datasets used for the analyses described in this manuscript were obtained from dbGaP at http://www.ncbi.nlm.nih.gov/sites/entrez?db:gap through dbGaP accession phs000138.v2.p1. The WHI datasets used for the analyses described in this manuscript were obtained from dbGaP at http://www.ncbi.nlm.nih.gov/sites/entrez?db:gap through dbGaP accession phs000200.v6.p2.

The Rotterdam study was funded by Erasmus Medical Center and Erasmus University, Rotterdam, Netherlands Organization for the Health Research and Development (ZonMw), the Ministry of Education, Culture and Science, the Ministry for Health, Welfare and Sports, the European Commission (DG XII) and the Municipality of Rotterdam, the Netherlands Organization of Scientific Research Netherlands Organisation for Scientific Research (NWO) Investments (175.010.2005.011 and 911-03-012 to KE, FR, and AGU); the Research Institute for Diseases in the Elderly (RIDE) (014-93-015 and RIDE2 to KE, FR, and AGU); and the Netherlands Genomics Initiative (NGI)/Netherlands Organization for Scientific Research (050-060-810 to KE, FR, and AGU). The Korean Genome Epidemiology Study (KoGES) was funded by the National Genome Research Institute, Korean Center for Disease Control and Prevention (2001-2003-348- 6111-221, 2004-347-6111-213 and 2005-347-2400-2440-215 to HJC, CSS, and NHC). The genotype data of KoGES were obtained from the Korean Genome Analysis Project (4845-301), which was funded by a grant from the Korea National Institute of Health (Korea Center for Disease Control, Ministry for Health, Welfare and Family Affairs, Cheongwon, Korea). The National Health and Medical Research Council Project Grant (511132 to the Anglo-Australasian Osteoporosis Genetics Consortium [AOGC]) and the National Health and Medical Research Council (Australia) Career Development Award (569807 to ELD). Funding of AOGC was also received from the Australian Cancer Research Foundation and Rebecca Cooper Foundation (Australia). TN is supported in part by a startup fund of Tulane University. LZ is partially supported by National Natural Science Foundation of China project (31100902). MAB is funded by a National Health and Medical Research Council (Australia) Senior Principal Research Fellowship. H-W D was partially supported by the Franklin D. Dickson/Missouri Endowment and is supported by the Edward G. Schlieder Endowment.

We are thankful for the generous support and assistance of Dr. Jian Li (Department of Biostatistics and Bioinformatics, Tulane University School of Public Health and Tropical Medicine) in the usage of data of four genome-wide association (GWA) cohorts (ie, FHS, IFS, WHI-AA, and WHI-HIS) from the National Center for Biotechnology Information (NCBI) database of genotypes and phenotypes (dbGaP). The AOGC thanks the research nurses involved in this study [Ms Barbara Mason and Ms Amanda Horne (Auckland), Ms Linda Bradbury and Ms Kate Lowings (Brisbane), Ms Katherine Kolk and Ms Rumbidzai Tichawangana (Geelong); Ms Helen Steane (Hobart); Ms Jemma Christie (Melbourne); and Ms Janelle Rampellini (Perth)]. The AOGC also acknowledges

gratefully technical support from Ms Kathryn Addison, Ms Marieke-Brugmans, Ms Catherine Cremen, Ms Johanna Hadler and Ms Karena Pryce. We thank Rongrong Zhang (Department of Cell and Molecular Biology, Tulane University School of Science and Engineering) for her valuable technical assistance.

Authors' roles: Study design: TN, NL, XY, MZ, SX, and HWD. Study conduct: TN, NL, XY, MZ, LZ, YFP, SX, and HWD. Data collection: HJC, PJL, MAB, HS, HH, SL, XDC, LJT, TLY, YG, NHC, JS, YFG, GCN, RLP, JAE, GJ, PNS, QT, XZZ, ELD, AGU, CSS, SX, and HWD. Data analysis: TN, NL, XY, MZ, LZ, YFP, HH, and XF. Materials contribution: SX, HWD. Drafting manuscript: TN, NL, MZ, SX, and HWD. Approving final version of manuscript: TN, NL, MZ, MAB, AGU, CSS, SX, and HWD. MAB, AGU, CSS, and HWD take responsibility for the integrity of data analyses of their respective conventional genome-wide association studies; TN, LZ, and HWD take responsibility for the integrity of data analyses of phosSNP-centric three-stage meta-analysis; and NL and SL take responsibility for the integrity of data analyses of in vitro experimental studies.

References

1. Kanis JA. Diagnosis of osteoporosis and assessment of fracture risk. Lancet. 2002;359(9321):1929–36.
2. National Osteoporosis Foundation. America's bone health: the state of osteoporosis and low bone mass in our nation. Washington, DC: National Osteoporosis Foundation; 2002.
3. Burge R, Dawson-Hughes B, Solomon DH, Wong JB, King A, Tosteson A. Incidence and economic burden of osteoporosis-related fractures in the United States, 2005–2025. J Bone Miner Res. 2007;22 (3):465–75.
4. WHO Study Group. Assessment of fracture risk and its application to screening for postmenopausal osteoporosis. Report of a WHO Study Group. World Health Organ Tech Rep Ser. 1994;843:1–129.
5. Benes H, Weinstein RS, Zheng W, et al. Chromosomal mapping of osteopenia-associated quantitative trait loci using closely related mouse strains. J Bone Miner Res. 2000;15(4):626–33.
6. Huang HD, Lee TY, Tzeng SW, et al. Incorporating hidden Markov models for identifying protein kinase-specific phosphorylation sites. J Comput Chem. 2005;26(10):1032–41.
7. Olsen JV, Vermeulen M, Santamaria A, et al. Quantitative phosphoproteomics reveals widespread full phosphorylation site occupancy during mitosis. Sci Signal. 2010;3(104):ra3.
8. Yan JX, Packer NH, Gooley AA, Williams KL. Protein phosphorylation: technologies for the identification of phosphoamino acids. J Chromatogr A. 1998;808(1–2):23–41.
9. Via A, Diella F, Gibson TJ, Helmer-Citterich M. From sequence to structural analyses in protein phosphorylation motifs. Front Biosci (Landmark Ed). 2011;16:1261–75.
10. Savas S, Ozcelik H. Phosphorylation states of cell cycle and DNA repair proteins can be altered by the nsSNPs. BMC Cancer. 2005;5:107.
11. Haraksingh RR, Snyder MP. Impacts of variation in the human genome on gene regulation. J Mol Biol. 2013;425(21):3970–7.
12. Cooper DN, Chen JM, Ball EV, et al. Genes, mutations, and human inherited disease at the dawn of the age of personalized genomics. Hum Mutat. 2010;31(6):631–55.
13. Kang HG, Lee SY, Jeon HS, et al. A functional polymorphism in CSF1R gene is a novel susceptibility marker for lung cancer among never-smoking females. J Thorac Oncol. 2014 Nov;9(11):1647–55.
14. Ozeki C, Sawai Y, Shibata T, et al. Cancer susceptibility polymorphism of p53 at codon 72 affects phosphorylation and degradation of p53 protein. J Biol Chem. 2011;286(20):18251–60.
15. Gentile S, Martin N, Scappini E, Williams J, Erxleben C, Armstrong DL. The human ERG1 channel polymorphism, K897T, creates a phosphorylation site that inhibits channel activity. Proc Natl Acad Sci U S A. 2008;105(38):14704–8.
16. Zhang X, Chen S, Zhang L, et al. Protective effect of KCNH2 single nucleotide polymorphism K897T in LQTS families and identification of novel KCNQ1 and KCNH2 mutations. BMC Med Genet. 2008;9:87.
17. Vazgiourakis VM, Zervou MI, Eliopoulos E, et al. Implication of VEGFR2 in systemic lupus erythematosus: a combined genetic and structural biological approach. Clin Exp Rheumatol. 2013;31(1): 97–102.
18. Ogus AC, Yoldas B, Ozdemir T, et al. The Arg753GLn polymorphism of the human toll-like receptor 2 gene in tuberculosis disease. Eur Respir J. 2004;23(2):219–23.
19. Xiong Y, Song C, Snyder GA, Sundberg EJ, Medvedev AE. R753Q polymorphism inhibits Toll-like receptor (TLR) 2 tyrosine phosphorylation, dimerization with TLR6, and recruitment of myeloid differentiation primary response protein 88. J Biol Chem. 2012; 287(45):38327–37.
20. Xue Y, Ren J, Gao X, Jin C, Wen L, Yao X. GPS 2.0, a tool to predict kinase-specific phosphorylation sites in hierarchy. Mol Cell Proteomics. 2008;7(9):1598–608.
21. Ren J, Jiang C, Gao X, et al. PhosSNP for systematic analyses of genetic polymorphisms that influence protein phosphorylation. Mol Cell Proteomics. 2010;9(4):623–34.
22. Gori F, Lerner U, Ohlsson C, Baron R. A new WNT on the bone: WNT16, cortical bone thickness, porosity and fractures. Bonekey Rep. 2015;4:669.
23. Zhu J, Qiu J, Magrane G, et al. Duplication of C7orf58, WNT16 and FAM3C in an obese female with a t(7;22)(q32.1;q11.2) chromosomal translocation and clinical features resembling Coffin-Siris Syndrome. PLoS One. 2012;7(12):e52353.
24. Fear MW, Kelsell DP, Spurr NK, Barnes MR. Wnt-16a, a novel Wnt-16 isoform, which shows differential expression in adult human tissues. Biochem Biophys Res Commun. 2000;278(3):814–20.
25. Movérare-Skrtic S, Henning P, Liu X, et al. Osteoblast-derived WNT16 represses osteoclastogenesis and prevents cortical bone fragility fractures. Nat Med. 2014 Nov;20(11):1279–88.
26. Panagiotou OA, Willer CJ, Hirschhorn JN, Ioannidis JP. The power of meta-analysis in genome-wide association studies. Annu Rev Genomics Hum Genet. 2013;14:441–65.
27. Reimand J, Wagih O, Bader GD. The mutational landscape of phosphorylation signaling in cancer. Sci Rep. 2013;3:2651.
28. Wang Z, Liu X, Yang BZ, Gelernter J. The role and challenges of exome sequencing in studies of human diseases. Front Genet. 2013;4:160.
29. Niu T, Liu N, Zhao M, et al. Identification of a novel FGFRL1 microRNA target site polymorphism for bone mineral density in meta-analyses of genome-wide association studies. Hum Mol Genet. 2015 Aug 15;24(16):4710–27.
30. Tabor HK, Risch NJ, Myers RM. Candidate-gene approaches for studying complex genetic traits: practical considerations. Nat Rev Genet. 2002;3(5):391–7.
31. Zhang L, Choi HJ, Estrada K, et al. Multistage genome-wide association meta-analyses identified two new loci for bone mineral density. Hum Mol Genet. 2014;23(7):1923–33.
32. Blom N, Gammeltoft S, Brunak S. Sequence and structure-based prediction of eukaryotic protein phosphorylation sites. J Mol Biol. 1999;294(5):1351–62.
33. Blom N, Sicheritz-Ponten T, Gupta R, Gammeltoft S, Brunak S. Prediction of post-translational glycosylation and phosphorylation of proteins from the amino acid sequence. Proteomics. 2004;4(6): 1633–49.
34. Reva B, Antipin Y, Sander C. Predicting the functional impact of protein mutations: application to cancer genomics. Nucleic Acids Res. 2011;39(17):e118.
35. Henikoff S, Henikoff JG. Amino acid substitution matrices from protein blocks. Proc Natl Acad Sci U S A. 1992;89(22):10915–9.
36. Ferrer-Costa C, Gelpi JL, Zamakola L, Parraga I, de la Cruz X, Orozco M. PMUT: a web-based tool for the annotation of pathological mutations on proteins. Bioinformatics. 2005;21(14):3176–8.
37. Thomas PD, Campbell MJ, Kejariwal A, et al. PANTHER: a library of protein families and subfamilies indexed by function. Genome Res. 2003;13(9):2129–41.

38. Bennett-Lovsey RM, Herbert AD, Sternberg MJ, Kelley LA. Exploring the extremes of sequence/structure space with ensemble fold recognition in the program Phyre. Proteins. 2008;70(3):611–25.
39. Kelley LA, Sternberg MJ. Protein structure prediction on the Web: a case study using the Phyre server. Nat Protoc. 2009;4(3):363–71.
40. Altschul SF, Madden TL, Schaffer AA, et al. Gapped BLAST and PSI-BLAST: a new generation of protein database search programs. Nucleic Acids Res. 1997;25(17):3389–402.
41. Estrada K, Styrkarsdottir U, Evangelou E, et al. Genome-wide meta-analysis identifies 56 bone mineral density loci and reveals 14 loci associated with risk of fracture. Nat Genet. 2012;44(5):491–501.
42. Bogdanova MA, Kostareva AA, Malashicheva AB. P342Lamin A/C mutations associated with different laminopathies affect differentiation of mesenchimal stem cells. Cardiovasc Res. 2014;103 Suppl 1: S62.
43. Alam I, Padgett LR, Ichikawa S, et al. SIBLING family genes and bone mineral density: association and allele-specific expression in humans. Bone. 2014;64:166–72.
44. Isaac J, Erthal J, Gordon J, et al. DLX3 regulates bone mass by targeting genes supporting osteoblast differentiation and mineral homeostasis in vivo. Cell Death Differ. 2014 Sep;21(9):1365–76.
45. Zhang L, Li J, Pei YF, Liu Y, Deng HW. Tests of association for quantitative traits in nuclear families using principal components to correct for population stratification. Ann Hum Genet. 2009;73(Pt 6): 601–13.
46. Johnson AD, Handsaker RE, Pulit SL, Nizzari MM, O'Donnell CJ, de Bakker PI. SNAP: a web-based tool for identification and annotation of proxy SNPs using HapMap. Bioinformatics. 2008;24(24):2938–9.
47. Brill LM, Xiong W, Lee KB, et al. Phosphoproteomic analyses of human embryonic stem cells. Cell Stem Cell. 2009;5(2):204–13.
48. Dyson HJ, Wright PE. Intrinsically unstructured proteins and their functions. Nat Rev Mol Cell Biol. 2005;6(3):197–208.
49. Neufeld EF, Muenzer J. The mucopolysaccharidoses. In: Scriver CR, Sly WS, Childs B, et al., editors. *The metabolic and molecular basis of inherited disease*. 8th ed. New York: McGraw-Hill 2001. p. 3421–52.
50. Wang D, Shukla C, Liu X, et al. Characterization of an MPS I-H knock-in mouse that carries a nonsense mutation analogous to the human IDUA-W402X mutation. Mol Genet Metab. 2010;99(1):62–71.
51. Ishizeki K, Saito H, Shinagawa T, Fujiwara N, Nawa T. Histochemical and immunohistochemical analyses of the mechanism of calcification of Meckel's cartilage during mandible development in rodents. J Anat. 1999;194(Pt 2):265–77.
52. Hartmann C. Skeletal development—Wnts are in control. Mol Cells. 2007;24(2):177–84.
53. Yang Y. Skeletal morphogenesis during embryonic development. Crit Rev Eukaryot Gene Expr. 2009;19(3):197–218.
54. Jiang Z, Von den Hoff JW, Torensma R, Meng L, Bian Z. Wnt16 is involved in intramembranous ossification and suppresses osteoblast differentiation through the Wnt/beta-catenin pathway. J Cell Physiol. 2014;229(3):384–92.
55. Medina-Gomez C, Kemp JP, Estrada K, et al. Meta-analysis of genome-wide scans for total body BMD in children and adults reveals allelic heterogeneity and age-specific effects at the WNT16 locus. PLoS Genet. 2012;8(7):e1002718.
56. Zheng HF, Tobias JH, Duncan E, et al. WNT16 influences bone mineral density, cortical bone thickness, bone strength, and osteoporotic fracture risk. PLoS Genet. 2012;8(7):e1002745.
57. Kemp JP, Medina-Gomez C, Estrada K, et al. Phenotypic dissection of bone mineral density reveals skeletal site specificity and facilitates the identification of novel loci in the genetic regulation of bone mass attainment. PLoS Genet. 2014;10(6):e1004423.
58. Dephoure N, Gould KL, Gygi SP, Kellogg DR. Mapping and analyses of phosphorylation sites: a quick guide for cell biologists. Mol Biol Cell. 2013;24(5):535–42.
59. Tyanova S, Cox J, Olsen J, Mann M, Frishman D. Phosphorylation variation during the cell cycle scales with structural propensities of proteins. PLoS Comput Biol. 2013;9(1):e1002842.
60. 1000 Genomes Project Consortium, Abecasis GR, Auton A, et al. An integrated map of genetic variation from 1,092 human genomes. Nature. 2012;491(7422):56–65.